VIBRATION ANALYSIS OF PRE-TWISTED ROTATING BEAMS

By

Tolga YILDIRIM

A Dissertation Submitted to the Graduate School in Partial Fulfillment of the Requirements for the Degree of

MASTER OF SCIENCE

Department: Mechanical Engineering
Major: Mechanical Engineering

Izmir Institute of Technology
Izmir, Turkey

May, 2003

We approve the thesis of **Tolga YILDIRIM**

Date of Signature

-- -------------------

Bülent Yardımoğlu

Asst. Professor of Mechanical Engineering

Thesis Advisor

-- -------------------

H. Seçil Altundağ Artem

Asst. Professor of Mechanical Engineering

-- -------------------

Engin Aktaş

Asst. Professor of Civil Engineering

-- -------------------

M. Barış Özerdem

Assoc. Professor and Chairman of the Department of Mechanical Engineering

ACKNOWLEDGEMENTS

The present work developed during my activity as a research assistant in the Department of Mechanical Engineering at Izmir Institute of Technology, Izmir.

First and foremost, I wish to thank my advisor Asst. Prof. Dr. Bülent Yardimoglu, who made it possible for me to write this thesis. I consider myself lucky to have two valuable years working with him.

For creating a pleasant working atmosphere I would like to thank the faculty members and research assistants at the Department of Mechanical Engineering. For their patience and friendships special thanks to the research assistants Ahmet Kaan Toksoy, Nurdan Yildirim, Pinar Ilker Alkan, Farah Tatar, Adil Caner Sener, Abdullah Berkan Erdogmus and Orhan Ekren, with whom I shared the same office at different times.

Last but not least, I would like to thank the administrative personnel Deniz Demirli and Aycin Bermant Ercan, from whom in one way or another I received help during my activity as a research assistant in the Department of Mechanical Engineering at Izmir Institute of Technology.

Izmir, May 2003 Tolga Yıldırım

ABSTRACT

A new linearly pretwisted rotating Timoshenko beam element, which has two nodes and four degrees of freedom per node, is developed and subsequently used for vibration analysis of pretwisted beams with uniform rectangular cross-section. First, displacement functions based on two coupled displacement fields (the polynomial coefficients are coupled through consideration of the differential equations of equilibrium) are derived for pretwisted beams. Next, the stiffness and mass matrices of the finite element model are obtained by using the energy expressions. Finally, the natural frequencies of pretwisted rotating Timoshenko beams are obtained and compared with previously published both theoretical and experimental results to confirm the accuracy and efficiency of the present model. The new pretwisted Timoshenko beam element has good convergence characteristics and excellent agreement is found with the previous studies.

ÖZ

İki düğümlü ve sekiz serbestlik dereceli yeni bir doğrusal burulmuş dönen Timoshenko çubuğu sonlu elemanı geliştirilmiş ve düzgün dikdörtgen kesitli önburulmalı çubukların titreşim analizinde kullanılmıştır. İlk olarak, yanal yerdeğiştirmeleri iki düzlemde bağlaşık olan önburulmalı çubuklar için yerdeğiştirme fonksiyonları (polinom sabitleri, sözü geçen diferansiyel denge denklemlerinde bağlaşık olan) türetilmiştir. Sonra, enerji ifadeleri kullanılarak sonlu eleman modelinin kütle ve direngenlik matrisleri elde edilmiştir. Son olarak da oluşturulan modelin doğruluğunu ve yeterliğini kanıtlamak için önburulmalı dönen Timoshenko çubukların doğal frekansları elde edilmiş ve daha önce yayınlanmış teorik ve deneysel sonuçlarla karşılaştırılmıştır. Oluşturulan yeni önburulmalı Timoshenko çubuk elemanı iyi yakınsama karakteristiği ve önceki çalışmalarla mükemmel bir uyuşma göstermiştir.

TABLE OF CONTENTS

LIST OF FIGURES

LIST OF TABLES

NOMENCLATURE

$\{a\}$	independent coefficient vector
a_0, a_1, a_2, a_3	polynomial coefficients of the linear displacement in xz plane
A	cross-sectional area of the beam
b_0, b_1, b_2, b_3	polynomial coefficients of the linear displacement in yz plane
b	breadth of the beam
c_0, c_1, c_2	polynomial coefficients of the angular displacement about the x axis
$\{d\}$	dependent coefficient vector
d_0, d_1, d_2	polynomial coefficients of the angular displacement about the y axis
E	modulus of elasticity
G	modulus of rigidity
h	depth of the beam
I_{xx}, I_{yy}	area moments of inertia of the cross-section about xx and yy axes
I_{xy}	product moment of inertia of the cross-section about xx-yy axes
$I_{x'x'}$, $I_{y'y'}$	area moments of inertia of the cross-section about x'x' and y'y' axes
k	shear coefficient
$[K_e]$	element stiffness matrix
L	length of the beam
$m(z)$	mass of the beam according to the analysed nodal coordinate
m_o	total mass of the beam
M_x, M_y	bending moments about x and y axes
$[M_e]$	mass matrix
$P(z)$	Axial force
$\{q_e\}$	element displacement vector

$[S_e]$	geometric stiffness matrix
T	kinetic energy
u	linear displacement in xz plane
U	strain energy
v	linear displacement in yz plane
V	strain energy due to axial force
V_x, V_y	shear forces in x and y direction
w	rotational speed
x, y	principal axes through the centroid at root section
x', y'	principal axes through the centroid at any section
z	co-ordinate distance measured along beam
z_{el}	co-ordinate of the element from the hub
θ	twist angle per unit length
θ_x	angular displacement about the x axis
θ_y	angular displacement about the y axis
ρ	density
ϕ_0	initial pretwist angle of the finite element
ϕ	pretwist angle of the finite element
ψ_x, ψ_y	shear angles about x and y axes
Ω_0	fundamental natural circular frequency of a untwisted beam
Ω	natural circular frequency of a pretwisted beam
$(\dot{})$	differentiation with respect to time
$(')$	differentiation with respect to z

Chapter 1

INTRODUCTION

The day that Dr. Gustaf Patrik de Laval, a Swedish engineer presented his marine steam turbine to the World Columbian Exposition in 1893, marks the beginning of the era of high speeds in rotating machinery. In the 1920's the turbine industry designed machines to operate at substantially higher loads and at speeds above the lowest critical speed, and this introduced the modern-day rotor dynamics problems.

Figure 1.1 Steam turbine

Since the advent of steam turbines and their application in various sectors of industry, it is a common experience that blade failures are a major cause of breakdown in these machines. Blade failures due to fatigue are predominantly vibration related. When a rotor blade passes across the nozzles of the stator, it experiences fluctuating lift and moment forces repeatedly at a frequency given by the number of nozzles multiplied by the speed of the machine. The blades are very flexible structural members, in the sense that a significant number of their natural frequencies can be in the region of possible nozzle excitation frequencies.

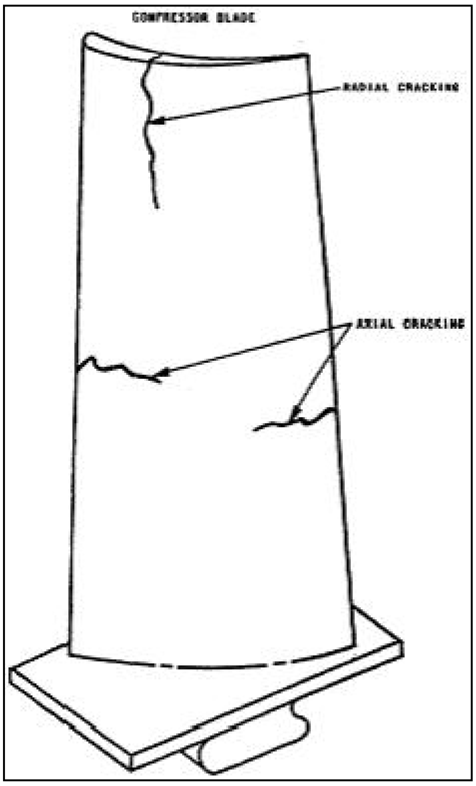

Figure 1.2 Typical blade cracks

It is very important for manufacturers of turbo machinery components to know the natural frequencies of the rotor blades, because they have to make sure that the turbine on which the blade is to be mounted does not have some of the same natural frequencies as the rotor blade. Otherwise, a resonance may occur in the whole structure of the turbine, leading to undamped vibrations, which may eventually wreck the whole turbine.

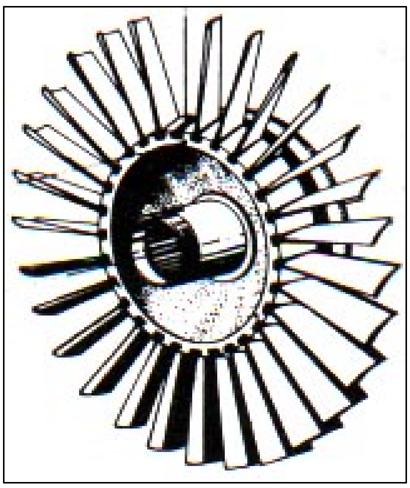

Figure 1.3 Schematic view of a part of a steam turbine

A single free standing blade can be considered as a pretwisted cantilever beam with a rectangular cross-section. Vibration characteristics of such a blade are always coupled between the two bending modes in the flapwise and chordwise directions and the torsion mode. The problem is also complicated by several second order effects such as shear deformations, rotary inertia, fiber bending in torsion, warping of the cross-section, root fixing and Coriolis accelerations.

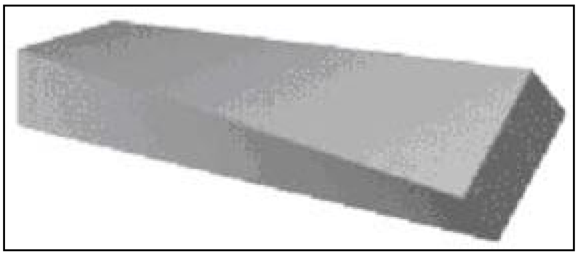

Figure 1.4 Pretwisted beam model

Many researchers analyzed uniform and twisted Timoshenko beams using different techniques: Exact solutions of Timoshenko's equation for simple supported uniform beams were given by Anderson [1]. The general equations of motion of a pretwisted cantilever blade were derived by Carnegie [2]. Then Carnegie [3] extended his study for the general equations of motion of a pretwisted cantilever blade allowing for torsion bending, rotary inertia and deflections due to shear. Dawson et al. [4] found the natural frequencies of pretwisted cantilever beams of uniform rectangular cross-section allowing for shear deformation and rotary inertia by the numerical integration of a set of first order simultaneous differential equations. They also made some experiments in order to obtain the natural frequencies for beams of various breadth to depth ratios and lengths ranging from 3 to 20 in and pretwist angle in the range 0°-90°. Gupta and Rao [5] used the finite element method to determine the natural frequencies of uniformly pretwisted tapered cantilever beams. Subrahmanyam et al. [6] applied the Reissner method and the total potential energy approach to calculate the natural frequencies and mode shapes of pretwisted cantilever blading including shear deformation and rotary inertia. Rosen [7] presented a survey paper as an extensive bibliography on the structural and dynamic aspects of pretwisted beams. Chen and Keer [8] studied the transverse vibration problems of a rotating twisted Timoshenko beam under axial loading and spinning about axial axis, and investigated the effects of the twist angle, rotational speed, and axial force on natural frequencies by finite element method. Chen and Ho [9] introduced the differential transform to solve the free vibration problems of a rotating twisted Timoshenko beam under axial loading. Lin et al. [10] derived the coupled governing differential equations and the general elastic boundary conditions for the coupled bending-bending forced vibration of a nonuniform pretwisted Timoshenko beam by Hamilton's principle. They used a modified transfer matrix method to study the dynamic behavior of a Timoshenko beam with arbitrary pretwist. Banerjee [11] developed a dynamic stiffness matrix and used for free vibration analysis of a twisted beam. Rao and Gupta [12] derived the stiffness and mass matrices of a rotating twisted and tapered Timoshenko beam element, and calculated the first four natural frequencies and mode shapes in bending-bending mode for cantilever beams. Narayanaswami and Adelman [13] showed that a straightforward energy minimization yields the correct stiffness matrix in displacement formulations when transverse shear effects are included. They also stated that in any finite element displacement formulation where transverse shear deformations are to be included, it is essential that the rotation of the normal (and not the derivative of transverse displacement) be retained as a nodal degree of freedom. Dawe [14] presented a Timoshenko beam finite element that has three nodes and two degrees of freedom per node, which are the lateral deflection and the cross-sectional rotation. The element properties were based on a coupled displacement field; the lateral deflection was interpolated as a quintic polynomial function and the cross-sectional rotation was linked to the deflection by specifying satisfaction of the moment equilibrium equation within the element. The effect of rotary inertia was included in "lumped" form at the nodes. Subrahmanyam et al. [15] analysed the lateral vibrations of a uniform rotating blade using Reissner and the total potential energy methods. Another vibration analysis of rotating pretwisted blades have been done by Yoo et al. [16]

The main purpose of this study is to create a new finite element model that shows a better convergence character and more accurate results with respect to the other finite element formulations in the literature to determine the natural frequencies of the blade structure. In order to reach this purpose, a new finite element model as an extension of Dawe's study to pretwisted Timoshenko beam is derived. Elastic and geometric stiffness and mass matrices of the element are obtained and used to reach the natural frequencies of the structure.

The results of our study show us that an excellent agreement with the previous studies has obtained.

Chapter 2

THEORY

There are two beam theories when dealing with transverse vibrations of prismatic beams:

1. Euler-Bernoulli beam theory (Classical beam theory)
2. Timoshenko beam theory.

2.1. Euler-Bernoulli beam theory

The Euler-Bernoulli beam equation arises from a combination of 4 distinct subsets of beam theory [23]:

1 Kinematic
2 Constitutive
3. Force resultant
4. Equilibrium

Kinematics describes how the beam's deflections are tracked. Out-of-plane displacement w, the distance the beam's neutral plane moves from its resting position, is usually accompanied by a rotation of the beam's neutral plane, defined as θ, and by a rotation of the beam's cross-section, χ.

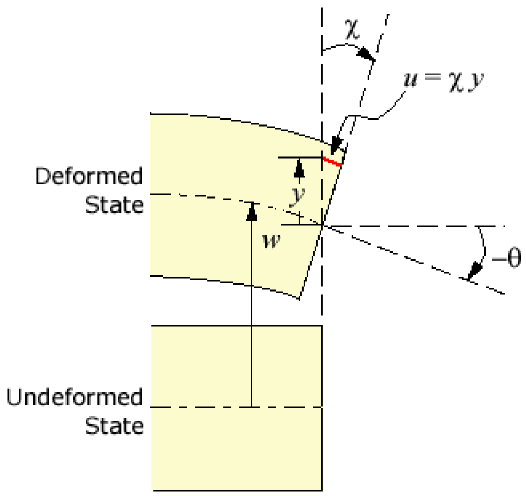

Figure 2.1 Kinematics of an Euler-Bernoulli beam

What we really need to know is the displacement in the x-direction across a beam cross-section, $u(x,y)$, from which we can find the direct strain $\varepsilon(x,y)$ by the equation,

$$\varepsilon = \frac{du}{dx} \tag{2.1}$$

To do so requires that we make a few assumptions on just how a beam cross-section rotates. For the Euler-Bernoulli beam, the assumptions were given by Kirchoff and dictate how the "normals" behave (normals are lines perpendicular to the beam's neutral plane and are thus embedded in the beam's cross-sections).

<u>Kirchoff Assumptions</u>

1. Normals remain straight (they do not bend)
2. Normals remain unstrecthed (they keep the same length)
3. Normals remain normal (they always make a right angle to the neutral plane)

With the normals straight and unstretched, we can safely assume that there is negligible strain in the y direction. Along with normals remaining normal to the neutral plane, we can make the x and y dependance in $u(x,y)$ explicit via a simple geometric expression,

$$u(x,y) = \chi(x)y \tag{2.2}$$

With explicit x dependance in u, we can find the direct strain throughout the beam,

$$\varepsilon(x,y) = \frac{d\chi}{dx}y \tag{2.3}$$

Finally, again with normals always normal, we can tie the cross-section rotation χ to the neutral plane rotation θ, and eventually to the beam's displacement w,

$$\chi = -\theta = -\frac{dw}{dx} \tag{2.4}$$

The **Constitutive** equation describes how the direct stress σ and direct strain ε within the beam are related. Direct means perpendicular to a beam cross-section; if we were to cut the beam at a given location, we would find a distribution of direct stress acting on the beam face.

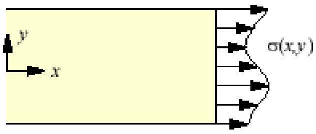

Figure 2.2 Direct stress distribution acting on the beam face

Beam theory typically uses the simple one-dimensional Hooke's equation,

$$\sigma(x, y) = E\varepsilon(x, y) \tag{2.5}$$

It can be noted that the stress and strain are functions of the entire beam cross-section (i.e. they can vary with y).

Force resultants are a convenient means for tracking the important stresses in a beam. They are analogous to the moments and forces of statics theory, in that their influence is felt throughout the beam (as opposed to just a local effect). Their convenience lies in them being only functions of x, whereas stresses in the beam are functions of x and y. If we were to cut a beam at a point x, we would find a distribution of direct stresses $\sigma(y)$ and shear stresses $\sigma_{xy}(y)$,

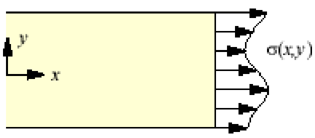

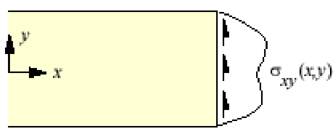

Figure 2.3 Direct and shear stress distributions on the beam cross-section

Each little portion of direct stress acting on the cross-section creates a moment about the neutral plane (y=0). Summing these individual moments over the area of the cross-section is the definition of the moment resultant M,

$$M(x) = \int\int y\sigma(x, y)dydz \tag{2.6}$$

where z is the coordinate pointing in the direction of the beam width (out of page). Summing the shear stresses on the cross-section is the definition of the shear resultant V,

$$V(x) = \int\int \sigma_{xy}(x, y)dydz \tag{2.7}$$

There is one more force resultant that we can define for completeness. The sum of all direct stresses acting on the cross-section is known as N,

$$N(x) = \int\int \sigma(x, y)dydz \tag{2.8}$$

$N(x)$ is the total direct force within the beam at some point x, yet it does not play a role in (linear) beam theory since it does not cause a displacement w. Instead, it plays a role in the axial displacement of rods and bars.

By inverting the definitions of the force resultants, we can find the direct stress distribution in the beam due to bending,

$$\sigma(x, y) = \frac{My}{I} \tag{2.9}$$

It is obvious that the bending stress in beam theory is linear through the beam thickness. The maximum bending stress occurs at the point furthest away from the neutral axis, y=c,

$$\sigma_{\max} = \frac{Mc}{I} \tag{2.10}$$

What about the other non-linear direct stresses shown acting on the beam cross-section? The average value of the direct stress is contained in N and does not contribute to beam theory. The remaining stresses (after the average and linear parts are subtracted away) are self-equilibrating stresses. By a somewhat circular argument, they are self-equilibrating precisely because they do not contribute to M or N, and therefore they do not play a global role. On the contrary, self-equilibrating loads are confined to have only a localized effect as mandated by Saint Venant's Principle.

[Saint-Venant's Principle can be stated as follows: If a set of self-equilibrating loads are applied on a body over an area of characteristic dimension d, the internal stresses resulting from these loads are only significant over a portion of the body of approximate characteristic dimension d. Note that this principle is rather vague, as it deals with ``approximate" characteristic dimensions. It allows qualitative rather than quantitative conclusions to be drawn.]

The **Equilibrium equations** describe how the beam carries external pressure loads with its internal stresses. Rather than deal with these stresses themselves, it is chosen to work with the resultants since they are functions of x only (and not of y).

To enforce equilibrium, consider the balance of forces and moments acting on a small section of beam,

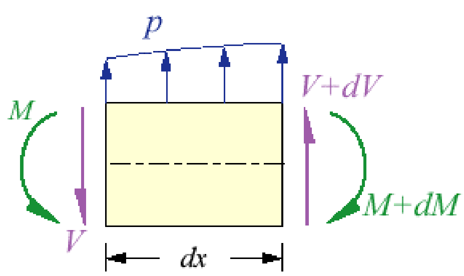

Figure 2.4 Force and moment equilibrium of the beam

Equilibrium in the y direction gives the equation for the shear resultant V,

$$\frac{dV}{dx} = -p \tag{2.11}$$

Moment equilibrium about a point on the right side of the beam gives the equation for the moment resultant M,

$$\frac{dM}{dx} = V \tag{2.12}$$

It can be noted that the pressure load p does not contribute to the moment equilibrium equation.

The outcome of each these segments is summarized here:

Kinematics: $\chi = -\theta = -\frac{dw}{dx}$

Constitutive: $\sigma(x, y) = E\varepsilon(x, y)$

Resultants: $M(x) = \int\int y\sigma(x, y)dydz$

$V(x) = \int\int \sigma_{xy}(x, y)dydz$

Equilibrium: $\frac{dM}{dx} = V$ $\frac{dV}{dx} = -p$

To relate the beam's out-of-plane displacement w to its pressure loading p, the results of the 4 beam sub-categories are combined in the order shown,

Kinematics -> Constitutive -> Resultants -> Equilibrium = Beam Equation

This hierarchy will be demonstrated by working backwards. First, the two equilibrium equations are combined to eliminate V,

$$\frac{d^2M}{dx^2} = -p \tag{2.13}$$

Next the moment resultant M is replaced with its definition in terms of the direct stress σ,

$$\frac{d^2}{dx^2}\left[\int\int y\sigma dydz\right] = -p \tag{2.14}$$

The constitutive relation is used to eliminate σ in favour of the strain ε, and then kinematics is used to replace ε in favour of the normal displacement w,

$$\frac{d^2}{dx^2}\left[E\int\int y\varepsilon dydz\right]=-p \qquad \frac{d^2}{dx^2}\left[E\frac{d\chi}{dx}\int\int y^2dydz\right]=-p$$

$$\frac{d^2}{dx^2}\left[E\frac{d^2w}{dx^2}\int\int y^2dydz\right]=p \tag{2.15}$$

As a final step, recognizing that the integral over y^2 is the definition of the beam's area moment of inertia I,

$$I=\int\int y^2dydz \tag{2.16}$$

allows us to arrive at the Euler-Bernoulli beam equation,

$$\frac{d^2}{dx^2}\left[EI\frac{d^2w}{dx^2}\right]=p \tag{2.17}$$

2.2. Timoshenko beam theory

Flexural wave speeds are much lower than the speed of either longitudinal or torsional waves. Therefore flexural wavelengths which are less than ten times the cross-sectional dimensions of the beam will occur at much lower frequencies. This situation occurs when analysing deep beams at low frequencies and slender beams at higher frequencies. In these cases, deformation due to transverse shear and kinetic energy due to rotation of the cross-section become important. In developing energy expressions which include both shear deformation and rotary inertia, the assumption that plane sections which are normal to the undeformed centroidal axis remain plane after bending, will be retained. However, it will no longer be assumed that these sections remain normal to the deformed axis [22].

The classical Euler-Bernoulli theory predicts the frequencies of flexural vibration of the lower modes of slender beams with adequate precision. However, because in this theory the effects of transverse shear deformation and rotary inertia are neglected the errors associated with it become increasingly large as the beam depth increases and as the wavelength of vibration decreases.

Timoshenko, a highly qualified engineer from Russia but had worked for an US turbine company Westinghouse, had made the corrections to the classical beam theory and developed the energy expressions which include both shear deformation and rotary inertia effects.

2.2.1 Kinematics

We consider a prismatic beam, symmetric cross-section with respect to (w.r.t.) z-axis (Figure 2.5).

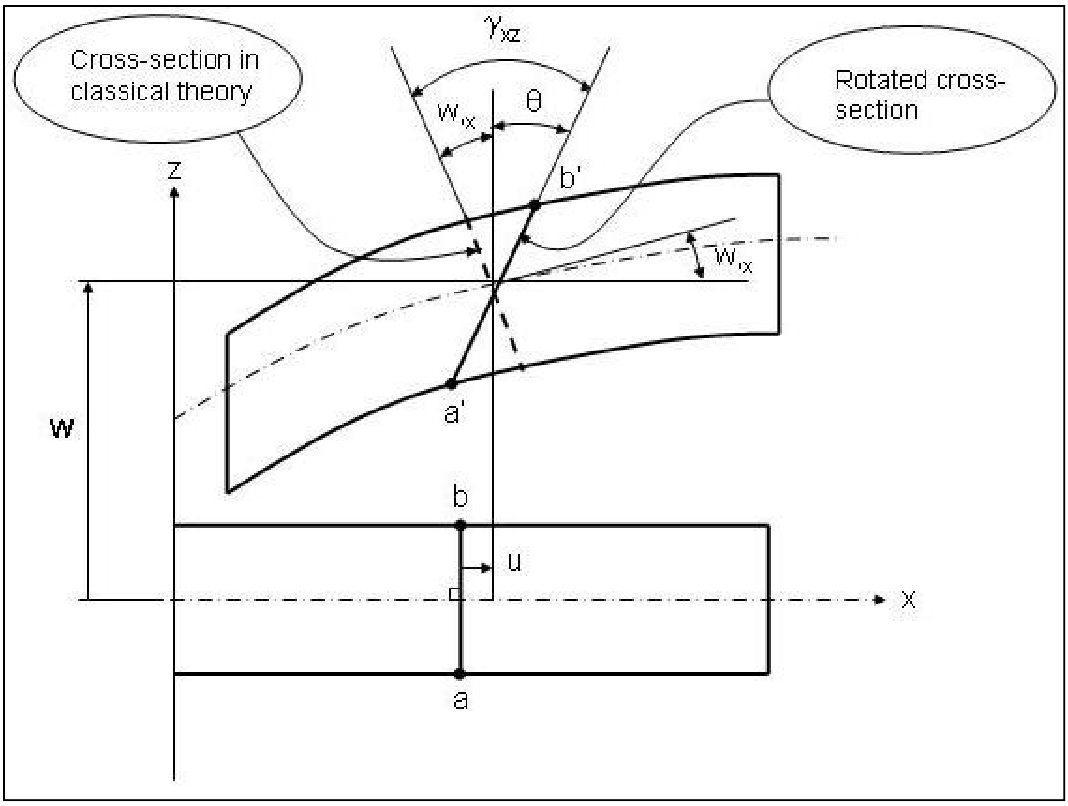

Figure 2.5 Kinematics of the Timoshenko Beam Theory

Apply $T_z(x, z = h/2)$ traction (Figure 2.6), uniform along y-direction, so that the applied transverse load will be,

$$g(x) = bT_z(x, h/2) \tag{2.18}$$

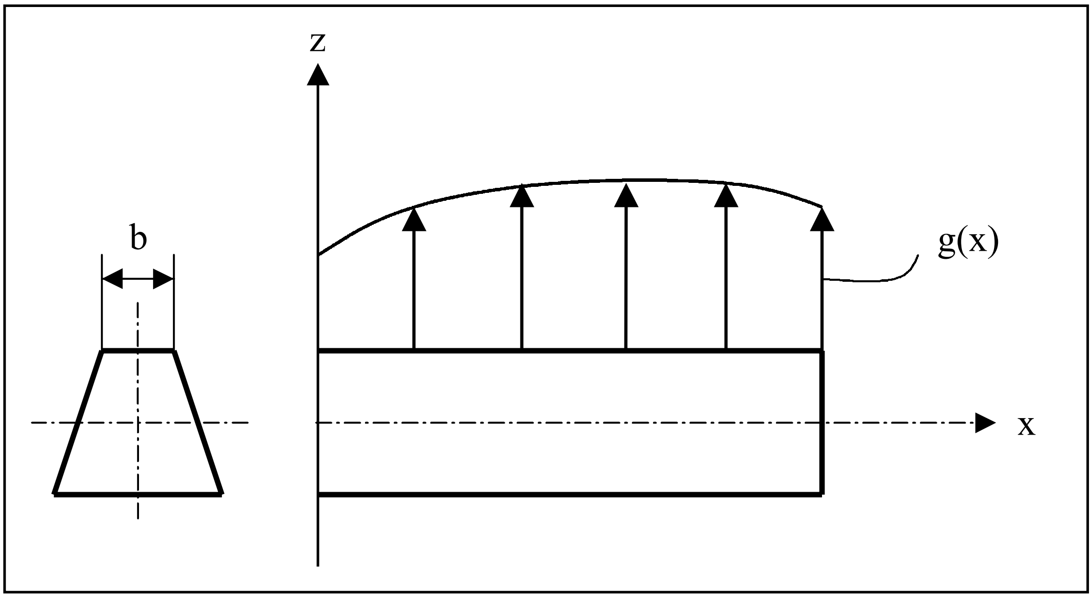

Figure 2.6 Application of uniform traction along y-direction

Assumptions

(1) Plane sections such as ab, originally normal to the centerline of the beam in the undeformed geometry, remain plane but not necessarily normal to the centerline in the deformed state.

(2) The cross-sections do not stretch or shorten, i.e., they are assumed to act like rigid surfaces.

(3) All displacements and strains are small, i.e., $w << h$, $\varepsilon_{ij} = 1/2\left(u_{i,j} + u_{j,i}\right)$

Assumption (2) implies that;

$$u_z = w(x) \text{ or } \varepsilon_{zz} = u_{z,z} = 0 \tag{2.19}$$

Assumption (1) implies that there exist constant (through the thickness) shear strains, i.e.,

$$\gamma_{xz} = \gamma_{xz}(x) \neq 0 \tag{2.20}$$

Now, writing down the shear strain in the x-z plane

$$\gamma_{xz} = u_{x,z} + u_{z,x} = u_{x,z} + w_{,x} \tag{2.21}$$

Now, solving Equation (2.21) for $u_{x,z}$

$$u_{x,z} = \gamma_{xz} - w_{,x} \tag{2.22}$$

and integrating w.r.t. z

$$u_x = z(\gamma_{xz} - w_{,x}) + f(x) \tag{2.23}$$

Evaluating u_x at the centerline z = 0 we have;

$$u_x(x, z = 0) = f(x) = u(x) \tag{2.24}$$

where $u(x)$ denotes displacement in the x-direction of any point on the centerline.

Replacing $f(x) = u(x)$ into Equation (2.23) we have;

$$u_x(x, z) = u(x) + z(\gamma_{xz} - w_{,x}) \tag{2.25}$$

where we note that $\gamma_{xz} = \gamma_{xz}(x)$ and $w = w(x)$.

Now introducing a variable called the bending rotation, $\theta(x)$, we can write

$$\theta(x) = \gamma_{xz} - w_{,x} \tag{2.26}$$

from which

$$\gamma_{xz} = w_{,x} + \theta \tag{2.27}$$

and Equation (2.25) becomes

$$u_x(x, z) = u + z\theta \tag{2.28}$$

and

$$u_z(x,z) \approx w(x) \tag{2.29}$$

Equations (2.28) and (2.29) represent the components of the displacement vector $\{u\}=\{u_x\, u_z\}$ of the Timoshenko beam. (It is noted as before that $u_y = 0$, i.e., all deformations along y-axis are neglected).

2.2.2 Strain – Displacement Relations

The only nonzero strains are;

$$\varepsilon_{xx} = u_{x,x} = u_{,x} + z\theta_{,x} = \varepsilon_{x0} + zk_{x0} \tag{2.30}$$

where

$\varepsilon_{x0} = u_{,x}$ (centerline axial strain)

and $k_{x0} = \theta_{,x}$ (bending curvature) (2.31)

and the transverse shear strain

$$\gamma_{xz} = w_{,x} + \theta \tag{2.32}$$

<u>Hooke's Law (Stress-Strain Relations)</u>

$$\sigma_{xx} = E\varepsilon_{xx} + \underline{\nu\left(\sigma_{yy} + \sigma_{zz}\right)} \tag{2.33}$$

$$\tau_{xz} = G\gamma_{xz} \tag{2.34}$$

The underlined term is generally neglected since it is much smaller than the first term. We then have:

$$\sigma_{xx} = E\varepsilon_{xx} = E(\varepsilon_{x0} + zk_{x0}) = E(u_{,x} + z\theta_{,x}) \tag{2.35}$$

$$\tau_{xz} = G\gamma_{xz} = G(w_{,x} + \theta) \tag{2.36}$$

2.2.3 Equilibrium Equations

The following integrals are defined:

$$N_x = \iint_A \sigma_{xx} dA \tag{2.37}$$

$$V_x = \iint_A \tau_{xz} dA \tag{2.38}$$

$$M_x = \iint_A \sigma_{xx} z dA \tag{2.39}$$

where N_x is the axial force, V_x is the shear force and M_x is the bending moment. The application of Principles of Virtual Work results the following equilibrium equations in the range $0 < x < L$ for the Timoshenko beam:

$$N_{x,x} = 0 \tag{2.40}$$

$$V_{x,x} + g = 0 \tag{2.41}$$

$$M_{x,x} - V_x = 0 \tag{2.42}$$

These three equations can be simplified further,
If we differentiate Equation (2.42) w.r.t. x and substitute Equation (2.41) into Equation (2.42):

$$M_{x,xx} + g = 0 \text{ (bending)} \tag{2.43}$$

$$N_{x,x} = 0 \text{ (axial)} \tag{2.44}$$

also, Equation (2.42) gives:

$$V_x = M_{x,x} \text{ (bending)} \tag{2.45}$$

2.2.4 Constitutive Equations

With reference to Equation (2.37),

$$N_x = \iint_A \sigma_{xx} dA = \iint_A E(u_{,x} + z\theta_{,x})dA$$

$$N_x = EAu_{,x} = EA\varepsilon_{x0} \tag{2.46}$$

$$M_x = \iint_A \sigma_{xx} z dA = \iint_A Ez(u_{,x} + z\theta_{,x})dA$$

$$M_x = EIk_{x0} = EI\theta_{,x} \tag{2.47}$$

$$I = \iint_A z^2 dA$$

Shear force:

Substituting Equation (2.36) into Equation (2.38) yields

$$V_x = \iint_A G\gamma_{xz} dA \cong k^2 GA\gamma_{xz} \tag{2.48}$$

where

GA = Shear rigidity

k^2 = nondimensional coefficient, referred to as a shear correction factor.

Bending Equilibrium Equations in terms of the Kinematic Variables of Timoshenko Beam Theory

Substituting the constitutive Equations (2.47) and (2.48) into Equations (2.41) and (2.42) gives:

$$\frac{d}{dx}\left[k^2 GA(w_{,x} + \theta)\right] + g(x) = 0 \tag{2.49}$$

$$\frac{d}{dx}(EI\theta_{,x}) - k^2 GA(w_{,x} + \theta) = 0 \tag{2.50}$$

Assuming GA and EI are constant, the above two equations can be readily reduced to a single equation in terms of w only, i.e.,

$$EIw^{(4)} + \left(\frac{EI}{k^2 GA} \right) g_{,xx} = g \tag{2.51}$$

The strain energy stored in the element is the sum of the energies due to bending and shear deformation; which is given by

$$U = 0.5 \int_V \sigma_x \varepsilon_x dV + 0.5 \int_V \tau_{xy} \gamma_{xy} dV \tag{2.52}$$

The kinetic energy of the straight beam consists of kinetic energy of translation and kinetic energy of rotation which is expressed as

$$T = 0.5 \int_0^L \rho A \dot{w}^2 dx + 0.5 \int_0^L \rho I \dot{\theta}^2 dx \tag{2.53}$$

2.3 Equations for pretwisted Timoshenko beam

The elastic potential energy of the pretwisted Timoshenko beam is given as [3];

$$U = 0.5 \int_0^L \left\{ E\left(I_{xx} \theta_x'^2 + 2 I_{xy} \theta_x' \theta_y' + I_{yy} \theta_y'^2 \right) + kAG\left(\left(u' - \theta_y\right)^2 + \left(v' - \theta_x\right)^2 \right) \right\} dz \tag{2.54}$$

where, the symbol " $'$ " represents differentiation with respect to z which is the longitudinal axis of the beam. The kinetic energy of the pretwisted thick beam is given as follows [3];

$$T = 0.5 \int_0^L \rho \left\{ A\left(\dot{u}^2 + \dot{v}^2 \right) + \left(I_{xx} \dot{\theta}_x^{\,2} + 2 I_{xy} \dot{\theta}_x \dot{\theta}_y + I_{yy} \dot{\theta}_y^{\,2} \right) \right\} dz \tag{2.55}$$

The differential equations of motion of the pretwisted beam with uniform rectangular cross-section are given as follows [3, 4];

$$\frac{d}{dz}(M_x)-V_y=I_{xx}\rho\ddot{\theta}_x, \qquad \frac{d}{dz}(M_y)-V_x=I_{yy}\rho\ddot{\theta}_y \qquad (2.56, 2.57)$$

$$\frac{d}{dz}(V_x)=\rho A\ddot{u}, \qquad \frac{d}{dz}(V_y)=\rho A\ddot{v} \qquad (2.58, 2.59)$$

where

$$M_x=EI_{xx}\theta_x'+EI_{xy}\theta_y', \qquad M_y=EI_{yy}\theta_y'+EI_{xy}\theta_x' \qquad (2.60, 2.61)$$

$$V_x=kAG\psi_y, \qquad V_y=kAG\psi_x \qquad (2.62, 2.63)$$

in which

$$\psi_x=v'-\theta_x, \qquad \psi_y=u'-\theta_y \qquad (2.64, 2.65)$$

In the above equations; M_x and M_y represents bending moments about x and y axes, V_x and V_y represents shear forces in x and y directions, ψ_x and ψ_y represents shear angles about x and y axes.

Chapter 3

FINITE ELEMENT VIBRATION ANALYSIS

3.1 Introduction

The Finite Element Method (FEM) is a numerical procedure that can be used to obtain solutions to a large class of engineering problems involving stress analysis, heat transfer, electromagnetism, fluid flow and vibration and acoustics.

In FEM, a complex region defining a continuum is discretized into simple geometric shapes called finite elements (see Figure 3.1). The material properties and the governing relationships are considered over these elements and expressed in terms of unknown values at element corners, called nodes. An assembly process, duly considering the loading and constraints, results in a set of equations. Solution of these equations gives us the approximate behaviour of the continuum.

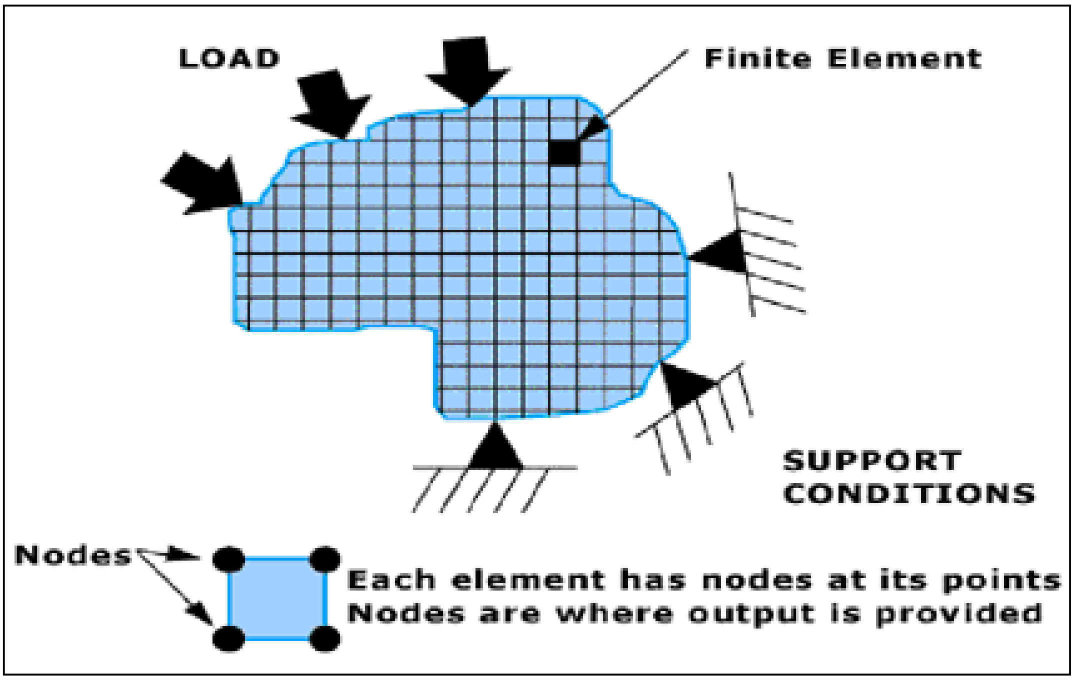

Figure 3.1 Description of the "finite element"

Basic ideas of the FEM originated from advances in aircraft structural analysis. The origin of the modern FEM may be traced back to the early 20th century, when some investigators approximated and modelled elastic continua using discrete equivalent elastic bars. However, Courant has been credited with being the first person to develop the FEM. He used piecewise polynomial interpolation over triangular subregions to investigate torsion problems in a paper published in 1943. The next significant step in the utilisation of Finite Element Method was taken by Boeing. In the 1950's Boeing, followed by others, used triangular stress elements to model airplane wings. But the term finite element was first coined and used by Clough in 1960. And since its inception, the literature on finite element applications has grown exponentially, and today there are numerous journals that are primarily devoted to the theory and application of the method.

3.2 Finite element vibration analysis

Here are the steps in finite element vibration analysis:

1. Discrete and select element type
2. Select a displacement function
3. Derive element stiffness and mass matrices
4. Assemble the element matrices and introduce BC's
5. Solve the eigenvalue problem and obtain the natural frequencies

A uniformly pretwisted constant cross-sectional beam is shown in Figure 3.2. Differential equations of the motion of pretwisted Timoshenko beam with uniform rectangular cross-section are given in the preceding chapter. The finite element model derived here is based on explicit satisfaction of the homogeneous form of Equations (2.56-2.59). In Equations (2.56-2.59), eliminating three parameters from the set $\{u, v, \theta_x, \theta_y\}$ in turn gives,

$$\frac{d^4u}{dz^4}=0, \qquad \frac{d^4v}{dz^4}=0, \qquad \frac{d^3\theta_x}{dz^3}=0, \qquad \frac{d^3\theta_y}{dz^3}=0 \qquad (3.1\text{- }3.4)$$

The Equations (3.1 - 3.4) result in an element with constant shear forces along its length, linear variation of moments, quadratic variation of cross-sectional rotations and cubic variation of transverse displacements. Therefore, the general solutions of these four equations are chosen as polynomials in z as follows:

$$u(z) = a_o + a_1 z + a_2 z^2 + a_3 z^3 \tag{3.5}$$

$$v(z) = b_o + b_1 z + b_2 z^2 + b_3 z^3 \tag{3.6}$$

$$\theta_x(z) = c_o + c_1 z + c_2 z^2 \tag{3.7}$$

$$\theta_y(z) = d_o + d_1 z + d_2 z^2 \tag{3.8}$$

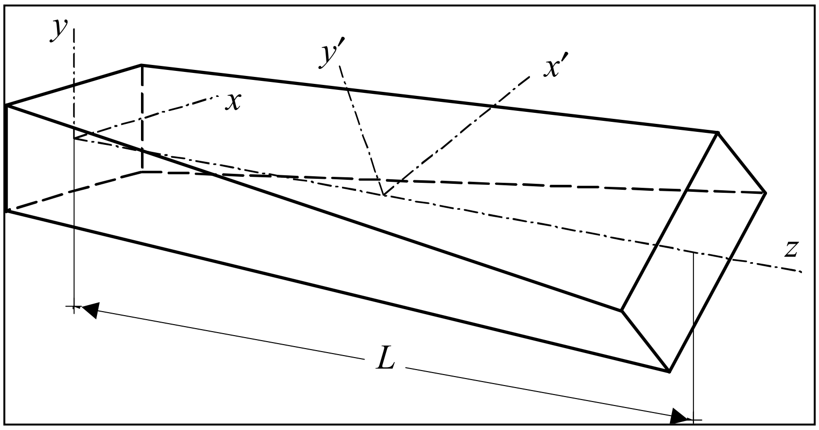

Figure 3.2 Uniformly pretwisted constant cross-sectional beam

Using homogeneous form of Equations (2.56-2.57), the relationships are obtained linking *u, v,* θ_x and θ_y in the form;

$$\frac{d}{dz}\left(EI_{xx}\theta_x' + EI_{xy}\theta_y'\right) + kAG\left(v' - \theta_x\right) = 0 \tag{3.9}$$

$$\frac{d}{dz}\left(EI_{yy}\theta_y' + EI_{xy}\theta_x'\right) + kAG\left(u' - \theta_y\right) = 0 \tag{3.10}$$

The area moments of inertia of the cross-section should be noted as follows:

$$I_{xx}(z) = I_{x'x'}\cos^2\phi(z) + I_{y'y'}\sin^2\phi(z)$$

$$I_{yy}(z) = I_{y'y'}\cos^2\phi(z) + I_{x'x'}\sin^2\phi(z) \tag{3.11}$$
$$I_{xy}(z) = 0.5\left(I_{x'x'} - I_{y'y'}\right)\sin 2\phi(z)$$
where $\phi(z) = \phi_0 + \theta z$

By using the Equations (3.5-3.10) the coefficients c_0, c_1, c_2, d_0, d_1 and d_2 can be expressed in terms of the coefficients a_0, a_1, a_2, a_3, b_0, b_1, b_2 and b_3 by equating coefficients of the powers of z. This procedure yields:

$$\begin{aligned}
c_o &= \beta_1 a_2 + \beta_2 a_3 + b_1 + \beta_3 b_2 + \beta_4 b_3, \\
c_1 &= \beta_5 a_3 + 2b_2 + \beta_6 b_3, \\
c_2 &= 3b_3 \\
d_0 &= a_1 + \beta_7 a_2 + \beta_8 a_3 + \beta_1 b_2 + \beta_2 b_3, \\
d_1 &= 2a_2 + \beta_9 a_3 + \beta_5 b_3, \\
d_2 &= 3a_3
\end{aligned} \tag{3.12}$$

where

$$\begin{aligned}
\beta_1 &= \frac{2E}{kAG} I'_{xy} \\
\beta_2 &= 6\left(\frac{E}{kAG}\right)^2 I'_{xy}\left(I'_{xx} + I'_{yy}\right) + \left(\frac{6E}{kAG}\right) I_{xy} \\
\beta_3 &= \frac{2E}{kAG} I'_{xx} \\
\beta_4 &= 6\left(\frac{E}{kAG}\right)^2 \left(I'^2_{xx} + I'^2_{xy}\right) + \left(\frac{6E}{kAG}\right) I_{xx} \\
\beta_5 &= \frac{6E}{kAG} I'_{xy} \\
\beta_6 &= \frac{6E}{kAG} I'_{xx} \\
\beta_7 &= \frac{2E}{kAG} I'_{yy}
\end{aligned} \tag{3.13}$$

$$\beta_8 = 6\left(\frac{E}{kAG}\right)^2 \left(I'^2{}_{yy} + I'^2{}_{xy}\right) + \left(\frac{6E}{kAG}\right) I_{yy}$$

$$\beta_9 = \frac{6E}{kAG} I'_{yy}$$

in which

$$\begin{aligned} I'_{xx} &= \theta\left(I_{y'y'} - I_{x'x'}\right)\sin 2\phi(z) \\ I'_{yy} &= \theta\left(I_{x'x'} - I_{y'y'}\right)\sin 2\phi(z) \\ I'_{xy} &= \theta\left(I_{x'x'} - I_{y'y'}\right)\cos 2\phi(z) \end{aligned} \tag{3.14}$$

It is convenient to express the Equation (3.12) in the matrix form:

$$\{d\} = [B]\{a\} \text{ or in open form } \begin{Bmatrix} c_0 \\ c_1 \\ c_2 \\ d_0 \\ d_1 \\ d_2 \end{Bmatrix} = \begin{bmatrix} 0 & 0 & \beta_1 & \beta_2 & 0 & 1 & \beta_3 & \beta_4 \\ 0 & 0 & 0 & \beta_5 & 0 & 0 & 2 & \beta_6 \\ 0 & 0 & 0 & 0 & 0 & 0 & 0 & 3 \\ 0 & 1 & \beta_7 & \beta_8 & 0 & 0 & \beta_1 & \beta_2 \\ 0 & 0 & 2 & \beta_9 & 0 & 0 & 0 & \beta_5 \\ 0 & 0 & 0 & 3 & 0 & 0 & 0 & 0 \end{bmatrix} \begin{Bmatrix} a_0 \\ a_1 \\ a_2 \\ a_3 \\ b_0 \\ b_1 \\ b_2 \\ b_3 \end{Bmatrix}$$

(3.15)

where $\{a\}$ and $\{d\}$ are named as independent and dependent coefficient vectors, respectively.

Similar procedure was applied to untwisted Timoshenko beam by Narayanaswami and Adelman [13] and Dawe [14].

3.3 Mass and stiffness matrices of the finite element

The new Timoshenko beam finite element has two nodes and four degrees of freedom per node, namely, two transverse deflections and two rotations (Figure 3.3). The element displacement vector can be written as:

$$\{q_e\}=\{u_1 \quad v_1 \quad \theta_{x1} \quad \theta_{y1} \quad u_2 \quad v_2 \quad \theta_{x2} \quad \theta_{y2}\}^T \tag{3.16}$$

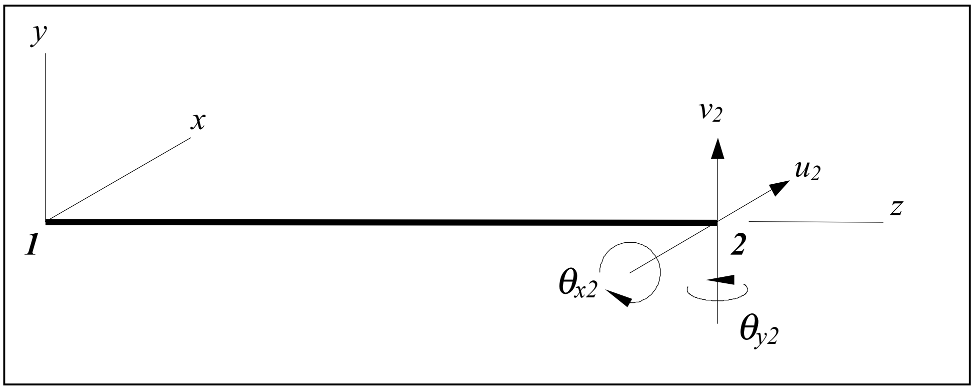

Figure 3.3 Finite element model

Then, by using Equations (3.5-3.8) and (3.12), $\{q_e\}$ can be expressed in terms of the independent coefficient vector as follows:

$$\{q_e\}=[C]\{a\} \tag{3.17}$$

$$\begin{Bmatrix} u_1 \\ v_1 \\ \theta_{x1} \\ \theta_{y1} \\ u_2 \\ v_2 \\ \theta_{x2} \\ \theta_{y2} \end{Bmatrix} = \begin{bmatrix} 1 & 0 & 0 & 0 & 0 & 0 & 0 & 0 \\ 0 & 0 & 0 & 0 & 1 & 0 & 0 & 0 \\ 0 & 0 & \beta_1 & \beta_2 & 0 & 1 & \beta_3 & \beta_4 \\ 0 & 1 & \beta_7 & \beta_8 & 0 & 0 & \beta_1 & \beta_2 \\ 1 & L & L^2 & L^3 & 0 & 0 & 0 & 0 \\ 0 & 0 & 0 & 0 & 1 & L & L^2 & L^3 \\ 0 & 0 & \beta_1 & (\beta_2+\beta_5 L) & 0 & 1 & (\beta_3+2L) & (\beta_4+\beta_6 L+3L^2) \\ 0 & 1 & (\beta_7+2L) & (\beta_8+\beta_9 L+3L^2) & 0 & 0 & \beta_1 & (\beta_2+\beta_5 L) \end{bmatrix} \begin{Bmatrix} a_0 \\ a_1 \\ a_2 \\ a_3 \\ b_0 \\ b_1 \\ b_2 \\ b_3 \end{Bmatrix}$$

The linear and angular displacement functions can be written by using the independent and dependent coefficient vectors, respectively, as follows:

$$u(z)=[P_u]\{a\}=\lfloor 1 \quad z \quad z^2 \quad z^3 \quad 0 \quad 0 \quad 0 \quad 0 \rfloor\{a\} \tag{3.18}$$

$$v(z)=[P_v]\{a\}=\lfloor 0 \quad 0 \quad 0 \quad 0 \quad 1 \quad z \quad z^2 \quad z^3 \rfloor\{a\} \tag{3.19}$$

$$\theta_x(z)=\lfloor P_{\theta_x} \rfloor\{d\}=\lfloor 1 \quad z \quad z^2 \quad 0 \quad 0 \quad 0 \rfloor\{d\} \tag{3.20}$$

$$\theta_y(z) = \lfloor P_{\theta_y} \rfloor \{d\} = \lfloor 0 \quad 0 \quad 0 \quad 1 \quad z \quad z^2 \rfloor \{d\} \tag{3.21}$$

Now, Equations (3.20) and (3.21) can be expressed by using Equation (3.15) as follows:

$$\theta_x(z) = \lfloor P_{\theta_x} \rfloor \, [B] \, \{a\} \tag{3.22}$$

$$\theta_y(z) = \lfloor P_{\theta_y} \rfloor \, [B] \, \{a\} \tag{3.23}$$

The elastic potential energy of the finite element in Figure 3.3 is written as [3]:

$$U = 0.5 \int_0^L \left\{ E\left(I_{xx}\theta_x'^2 + 2I_{xy}\theta_x'\theta_y' + I_{yy}\theta_y'^2 \right) + kAG\left((u' - \theta_y)^2 + (v' - \theta_x)^2 \right) \right\} dz \tag{3.24}$$

where, the symbol " ′ " represents differentiation with respect to z. Substituting Equations (3.11), (3.18), (3.19), (3.22) and (3.23) into Equation (3.24) gives

$$U = 0.5 \{ q_e \}^T [K_e] \{ q_e \} \tag{3.25}$$

where $[K_e]$ is the element stiffness matrix given by

$$[K_e] = \int_0^L \left\{ [C]^{-T} [k] [C]^{-1} \right\} dz \tag{3.26}$$

in which

$$\begin{aligned}
[k] = {} & [B]^T E \left\{ I_{xx}(z) \lfloor P'_{\theta_x} \rfloor^T \lfloor P'_{\theta_x} \rfloor + I_{yy}(z) \lfloor P'_{\theta_y} \rfloor^T \lfloor P_{\theta_y} \rfloor + I_{xy}(z) \left(\lfloor P'_{\theta_x} \rfloor^T \lfloor P'_{\theta_y} \rfloor + \lfloor P'_{\theta_y} \rfloor^T \lfloor P'_{\theta_x} \rfloor \right) \right\} [B] \\
& + kAG \left\{ \left([P'_u]^T [P'_u] + [P'_v]^T [P'_v] \right) + \left([B]^T \left(\lfloor P_{\theta_y} \rfloor^T \lfloor P_{\theta_y} \rfloor + \lfloor P_{\theta_x} \rfloor^T \lfloor P_{\theta_x} \rfloor \right) [B] \right) \right\} \\
& - kAG \left\{ \left([B]^T \left(\lfloor P_{\theta_y} \rfloor^T [P'_u] + \lfloor P_{\theta_x} \rfloor^T [P'_v] \right) \right) + \left(\left([P'_u]^T \lfloor P_{\theta_y} \rfloor + [P'_v]^T \lfloor P_{\theta_x} \rfloor \right) [B] \right) \right\}
\end{aligned} \tag{3.27}$$

In order to examine the effect of rotational speed on the natural frequencies, the system shown in Figure 3.4 is considered. The strain energy due to axial force can be written as follows:

$$V = \frac{1}{2}\int_0^l P(z)\left(u'^2 + v'^2\right)dz \tag{3.28}$$

where

$$P(z) = m(z)w^2\left(z_{el} + z\right) \tag{3.29}$$

and

$$m(z) = m_o - \mu\left(z_{el} + z\right) \tag{3.30}$$

in which m_o is the total mass of the beam and μ is the "mass/unit length" of the beam. Substituting the derivations of Equations (3.18) and (3.19) with the Equations (3.29) and (3.30) into (3.28) gives:

$$V = 0.5\{q_e\}^T[S_e]\{q_e\} \tag{3.31}$$

where $[S_e]$ is the element geometric stiffness matrix given by

$$[S_e] = [C]^{-T}\left[\int_0^l P(z)\left([P_u']^T[P_u'] + [P_v']^T[P_v']\right)dz\right][C]^{-1} \tag{3.32}$$

The kinetic energy of the pretwisted thick beam is given as follows [3]:

$$T = 0.5\int_0^L \rho\left\{A\left(\dot{u}^2 + \dot{v}^2\right) + \left(I_{xx}\dot{\theta}_x^{\ 2} + 2I_{xy}\dot{\theta}_x\dot{\theta}_y + I_{yy}\dot{\theta}_y^{\ 2}\right)\right\}dz \tag{3.33}$$

where the use of the overdot is a compact notation for differentiation with respect to time. Substituting Equations (3.11), (3.18), (3.19), (3.22) and (3.23) into Equation (3.33) gives

$$T = 0.5\{\dot{q}_e\}^T [M_e] \{\dot{q}_e\} \tag{3.34}$$

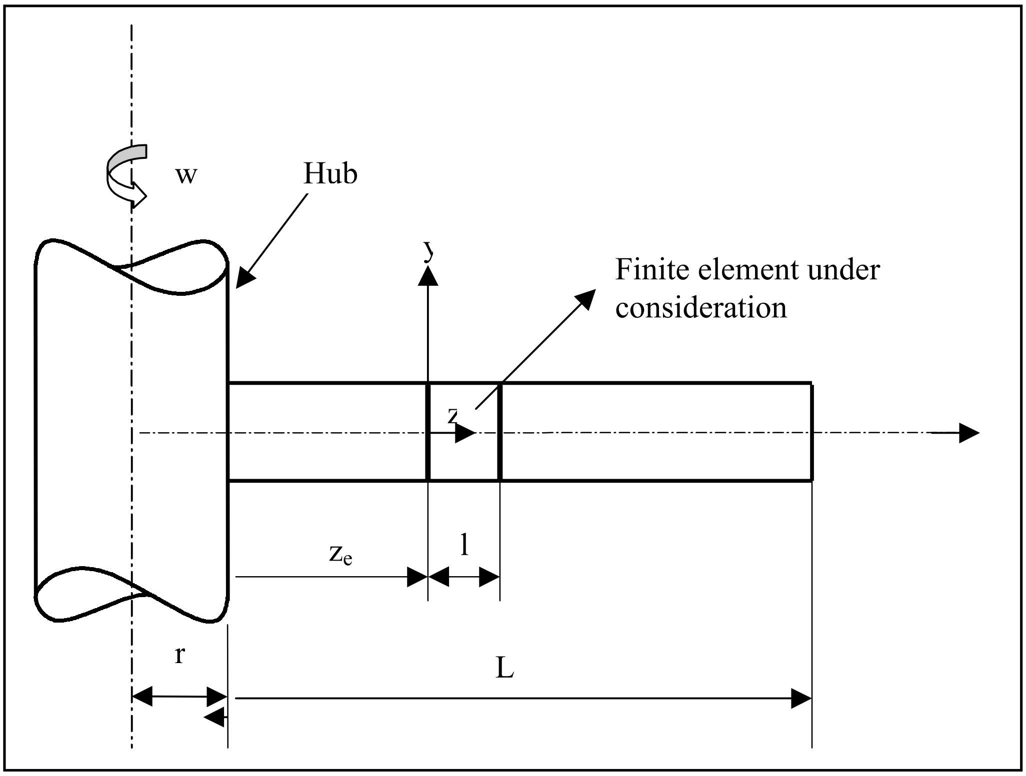

Figure 3.4 Model for rotation effect

where $[M_e]$ is the element mass matrix given by

$$[M_e] = \int_0^L \left\{ [C]^{-T} [m][C]^{-1} \right\} dz \tag{3.35}$$

in which

$$\begin{aligned}[m] &= \rho A\left(\lfloor \dot{P}_u \rfloor^T \lfloor \dot{P}_u \rfloor + \lfloor \dot{P}_v \rfloor^T \lfloor \dot{P}_v \rfloor \right) \\ &+ \rho\left\{ [B]^T \left(I_{xx}(z) \lfloor \dot{P}_{\theta_x} \rfloor^T \lfloor \dot{P}_{\theta_x} \rfloor + I_{xy}(z)\left(\lfloor \dot{P}_{\theta_x} \rfloor^T \lfloor \dot{P}_{\theta_y} \rfloor + \lfloor \dot{P}_{\theta_y} \rfloor^T \lfloor \dot{P}_{\theta_x} \rfloor \right) + I_{yy}(z) \lfloor \dot{P}_{\theta_y} \rfloor^T \lfloor \dot{P}_{\theta_y} \rfloor \right) [B] \right\}\end{aligned} \tag{3.36}$$

3.4 Numerical integration

In order to compute $[K_e]$, $[S_e]$ and $[M_e]$ in the Equations (3.26), (3.32) and (3.35), Gauss-Legendre 4-point numerical integration is used. The n-point approximation is given by the following formula [19];

$$I = \int_{-1}^{1} f(\xi)d\xi \approx w_1 f(\xi_1) + w_2 f(\xi_2) + . \quad . \quad . + w_n f(\xi_n) \tag{3.37}$$

where w_1, w_2, w_3 and w_4 are the weights and ξ_1, ξ_2, ξ_3 and ξ_4 are the sampling points or Gauss points. The idea behind Gaussian quadrature is to select the n Gauss points and n weights such that Equation (3.37) provides an exact answer for polynomials $f(\xi)$ of as large a degree as possible.

The Gauss points and weights for 4-point Gauss-Legendre numerical integration is given in Table 3.1. In our analysis the integration starts from 0 to the length of the finite element, so a modification should be needed for the Gauss points and weights [18].

$$I = \int_{a}^{b} f(\xi)d\xi \approx \sum_{i=1}^{n} \underline{w_i} f(\underline{\xi_i}) \tag{3.38}$$

$$\underline{w_i} = \frac{(b-a)}{2} w_i \tag{3.39}$$

$$\underline{\xi_i} = \frac{(a+b)}{2} + \frac{(b-a)}{2} \xi_i \tag{3.40}$$

Point number	Gauss points	Weights
1	-0.8611363116	0.3478548451
2	-0.3399810436	0.6521451549
3	0.3399810436	0.6521451549
4	0.8611363116	0.3478548451

Table 3.1 Gauss points and weights for 4-point Gaussian quadrature

3.5. Assembling of the element matrices

The global mass and stiffness matrices are obtained by assembling the element matrices given in Equations (3.26), (3.32) and (3.35). The assembling process is carried out by the computer program developed in MatLAB. The connectivity table for the 10 element solution is given in Table 3.2 to give an idea about how the computer connects the element matrices. Every node in an element has both a local coordinate and a global coordinate.

Element Number	Local Coordinates								
	1	**2**	**3**	**4**	**5**	**6**	**7**	**8**	
1	1	2	3	4	5	6	7	8	**Global Coordinates**
2	5	6	7	8	9	10	11	12	
3	9	10	11	12	13	14	15	16	
4	13	14	15	16	17	18	19	20	
5	17	18	19	20	21	22	23	24	
6	21	22	23	24	25	26	27	28	
7	25	26	27	28	29	30	31	32	
8	29	30	31	32	33	34	35	36	
9	33	34	35	36	37	38	39	40	
10	37	38	39	40	41	42	43	44	

Table 3.2 Connectivity Table

3.6. Determination of the natural frequencies

By using the well-known procedures of vibration analysis, the eigenvalue problem can be given as [17];

$$\left([K] - \Omega^2 [M]\right) \{q\} = 0 \tag{3.41}$$

where $\left[K\right]$ and $\left[M\right]$ are global stiffness (geometric stiffness matrix included) and mass matrices, respectively, and $\{q\}$ is global displacement vector, and Ω is the natural circular frequency. The eigenvalue problem given in Equation (3.41) is solved by using computer programs developed in MatLAB.

Chapter 4

RESULTS AND DISCUSSION

In order to validate the proposed finite element model for the vibration analysis of pretwisted Timoshenko beam, various numerical results are obtained and compared with available solutions in the published literature.

4.1. Simply supported untwisted beam

The first example to be considered is the case of lateral vibrations of a non-rotating untwisted rectangular cross-section beam with both ends simply supported. In Table 4.1, comparison of the analytical results obtained from closed-form solution derived by Anderson [1], finite element solution with 20 and 40 elements given by Chen and Keer [8] and the present model with 10 elements is made. Excellent agreement is observed. The physical properties of the beam are given in Table 4.1.

Mode	Anderson Analytical [1]	Chen, Keer FEM [8]		Present FEM 10 elements	Difference between Analytical and Present %
		20 elements	40 elements		
1	114,78	115,14	114,87	113,99	0,69
2	333,46	334,44	333,70	331,21	0,67
3	453,49	459,01	454,86	450,55	0,65
4	1000,38	1027,41	1007,03	995,81	0,46
5	1216,72	1229,63	1219,92	1211,76	0,41
Data: length of beam = 101.6 cm, width = 5.08 cm, thickness = 15.24 cm, shear coefficient = 5/6, E = 206.8 Gpa, G = 79.3 Gpa, mass density = 7860 kg/m^3.					

Table 4.1 Comparison of coupled bending-bending frequencies of an untwisted, simple supported rectangular cross-section beam

4.2. Cantilever pretwisted beam (twist angle = 45°)

The second example is concerned with a cantilever pretwisted beam treated experimentally by Carnegie [2] and by theoretical means by Lin et al. [10] and Subrahmanyam et al. [6]. The properties of the beam are given in Table 4.2. To show efficiency and convergence of the proposed model, the first four frequencies of the second example are calculated. For comparison, the present results as well as those given by other investigators are tabulated in Table 4.2. It is observed that the agreement between the present results and results of the other investigators is very good. The natural frequencies calculated by the proposed model converge very rapidly. Even when the number of the element is only 10, the present fundamental frequency is converged.

Number of element	Mode number			
	1	2	3	4
2	64,3	465,5	1087,7	1921,6
4	62,3	327,3	1041,7	1226,2
6	62,0	313,6	986,3	1179,2
8	61,9	309,3	965,4	1178,3
10	61,8	307,3	956,1	1181,9
12	61,8	306,3	951,2	1185,4
14	61,8	305,6	948,3	1188,1
16	61,8	305,3	946,6	1190,2
18	61,8	305,0	945,4	1191,7
20	61,8	304,8	944,5	1193,0
Lin et al. [10]	61,7	300,9	917,0	1175,1
Subrahmanyam et al. [6]	62,0	305,1	955,1	1214,7
Subrahmanyam et al. [6]	61,9	304,7	937,0	1205,1
Carnegie [2]	59,0	290,0	920,0	1110,0
Data: length of beam = 15.24 cm, breadth = 2.54 cm, depth = 0.17272 cm, shear coefficient = 0.847458, E = 206.85 Gpa, G = 82.74 Gpa, mass density = 7857.6 kg/m^3, twist angle = 45°.				

Table 4.2. Convergence pattern and comparison of the frequencies of a cantilever pretwisted uniform Timoshenko beam (Hz).

4.3. Cantilever pretwisted beam (various twist angle, length, breadth to depth ratio)

This example is considered to evaluate the present finite element formulation for the effects of related parameters (e.g. twist angle, length, breadth to depth ratio) on the natural frequencies of the pretwisted cantilever Timoshenko beams treated experimentally by Dawson et al. [4]. The natural frequencies are prescribed in terms of the frequency ratio Ω / Ω_0, where Ω is the natural frequency of pretwisted beam and Ω_0 is the fundamental natural frequency of untwisted beam. The natural frequency ratios for the first five modes of vibration are obtained for two groups of cantilever beams (Table 4.3) of uniform rectangular cross-section by using 10 elements.

		Length			
		7,62 cm	**15,24 cm**	**30,48 cm**	**50,8 cm**
b/d	8/1	x	x	x	x
	4/1	x	x	x	x
	2/1	x	x	x	x

Table 4.3. Two groups of cantilever beams for the analysis of the effect of various parameters on the natural frequencies.

First group includes the sets of beams of breadth 0.0254 m and length 0.3048 m and various breadth to depth ratios and pretwist angle in the range 0-90°. The results for first group are shown in Tables 4.4, 4.5, 4.6 and in Figures 4.1, 4.2, and 4.3.

Second group contains the sets of beams of breadth 0.0254 m and breadth to depth ratio 8/1 and length ranging from 0.0762 m to 0.508 m and pretwist angle in the range 0-90°. The results for second group are shown in Figures 4.1, 4.4, 4.5, and 4.6. It can easily be checked out from the Figures of the second group that the natural frequencies increase as the beam length decreases.

Twist Angle	Mode Numbers Frequency Ratio (b/d=8/1), Length=12 in 1	2	3	4	5	Analysis Types
0	1,0	6,3	8,0	17,5	34,3	Present (10 Elements)
30	1,0	5,3	9,4	17,1	34,0	
60	1,0	4,2	11,7	16,1	33,0	
90	1,0	3,4	12,8	16,3	31,7	
0	1,0	6,2	8,0	17,7	35,1	Chen, Keer [8] (25 Elements)
30	1,0	5,2	9,4	17,2	34,6	
60	1,0	4,2	11,7	16,5	33,6	
90	1,0	3,1	12,9	16,8	32,2	
0	1,1	6,4	7,7	17,2	34,0	Dawson et al. [4]
30	1,1	5,3	9,2	16,5	33,4	
60	1,1	4,2	11,3	15,7	32,3	
90	1,1	3,4	12,4	16,2	30,8	
0	1,0	6,1	7,8	17,3	34,1	Chen, Ho [9]
30	1,0	5,0	9,1	16,7	33,7	
60	1,0	4,3	11,6	16,1	32,7	
90	1,0	3,3	12,1	16,5	31,1	

Table 4.4 Result I for the first group of beams

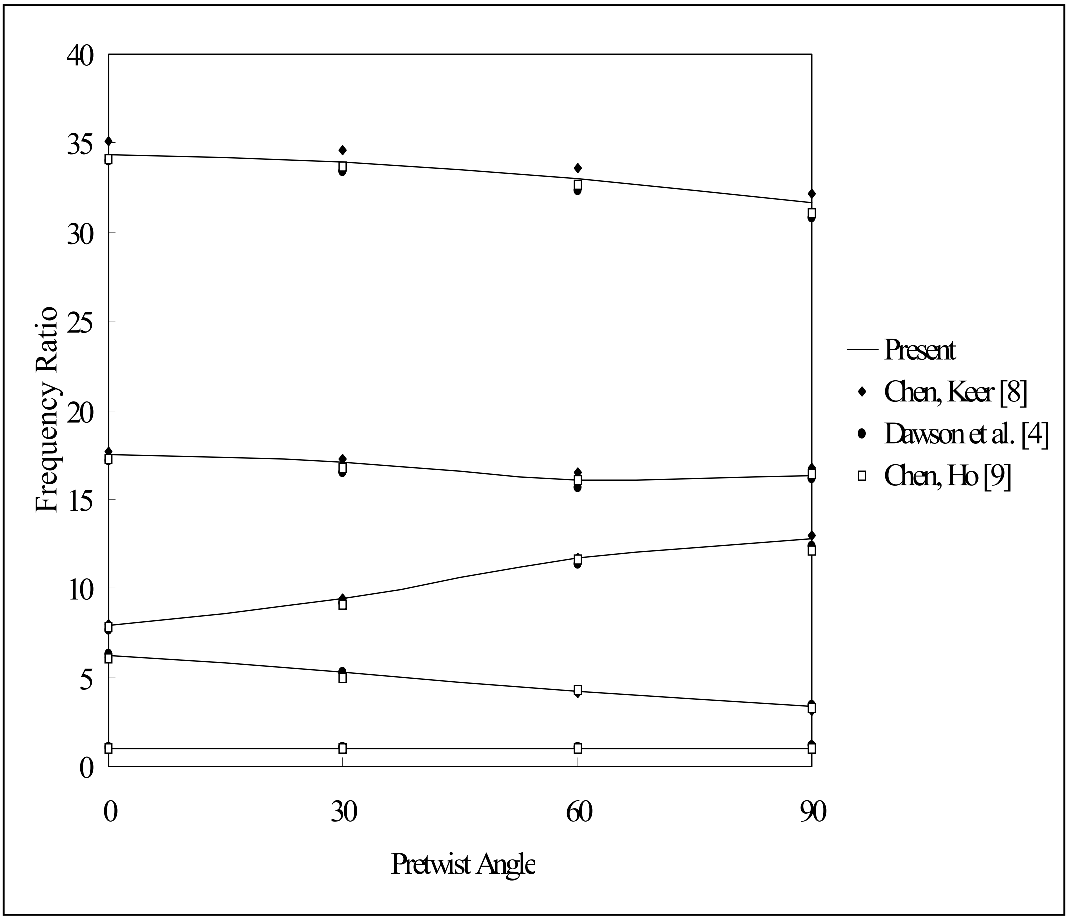

Figure 4.1. Frequency ratio vs twist angle. Length 30.48 cm, breadth 2.54 cm, b/h = 8/1.

Twist Angle	Mode Numbers					Analysis Types
	Frequency Ratio (b/d= 4/1), Length=12 in					
	1	2	3	4	5	
0	1,0	4,0	6,3	17,5	24,2	Present
30	1,0	3,7	6,7	16,6	25,4	
60	1,0	3,3	7,7	15,0	27,9	
90	1,0	2,8	8,9	13,5	29,4	
0	1,0	4,0	6,2	17,2	24,5	Dawson et al. [4]
30	0,9	3,6	6,3	16,4	25,2	
60	1,0	3,2	7,2	14,6	27,3	
90	0,9	2,8	8,3	13,2	28,9	

Table 4.5 Result II for the first group of beams

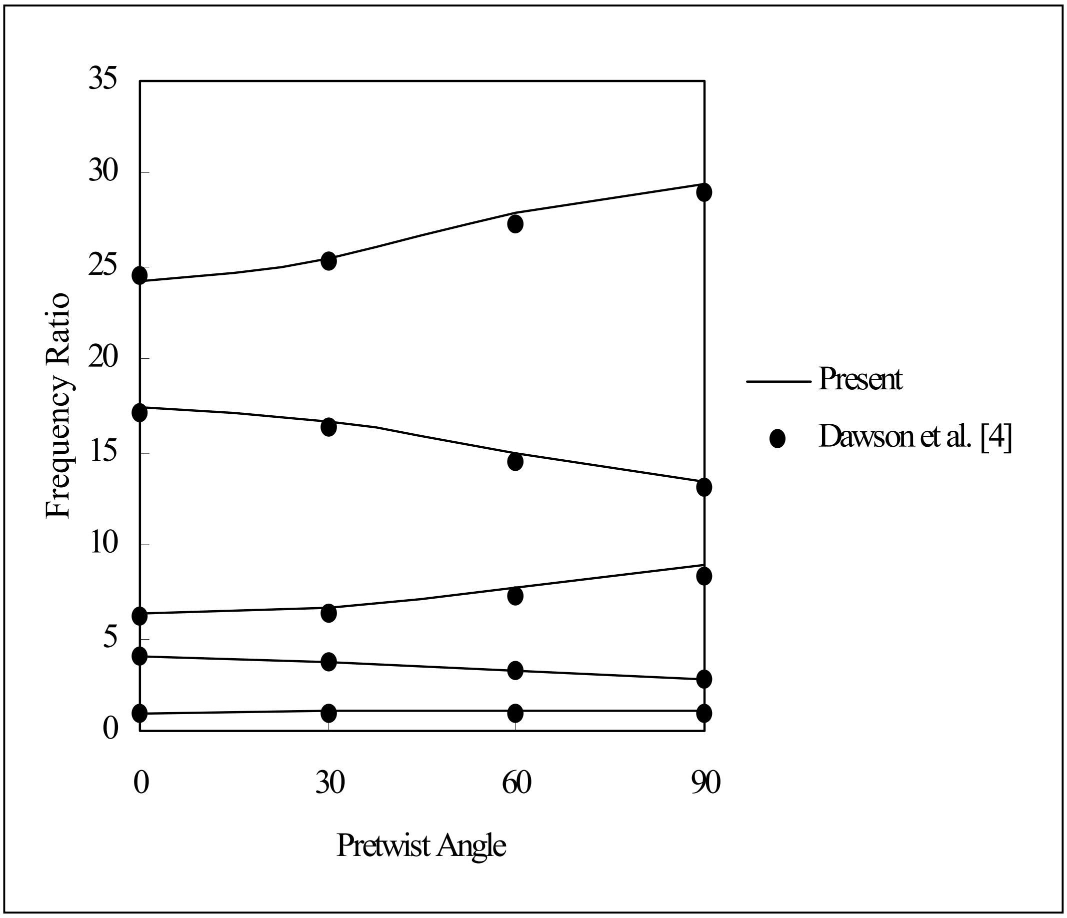

Figure 4.2. Frequency ratio vs twist angle. Length 30.48 cm, breadth 2.54 cm, b/h = 4/1.

Twist Angle	Mode Numbers					Analysis Types
	Frequency Ratio (b/d=2/1), Length=12 in					
	1	2	3	4	5	
0	1,0	2,0	6,2	12,1	17,2	Present
30	1,0	2,0	6,3	11,8	17,6	
60	1,0	1,9	6,5	11,2	18,6	
90	1,0	1,8	6,9	10,4	20,0	
0	1,0	2,0	6,0	11,6	16,3	Dawson et al. [4]
30	1,0	1,9	5,9	11,4	16,8	
60	1,0	1,7	6,2	10,7	18,0	
90	1,0	1,8	6,5	9,8	19,7	

Table 4.6 Result III for the first group of beams

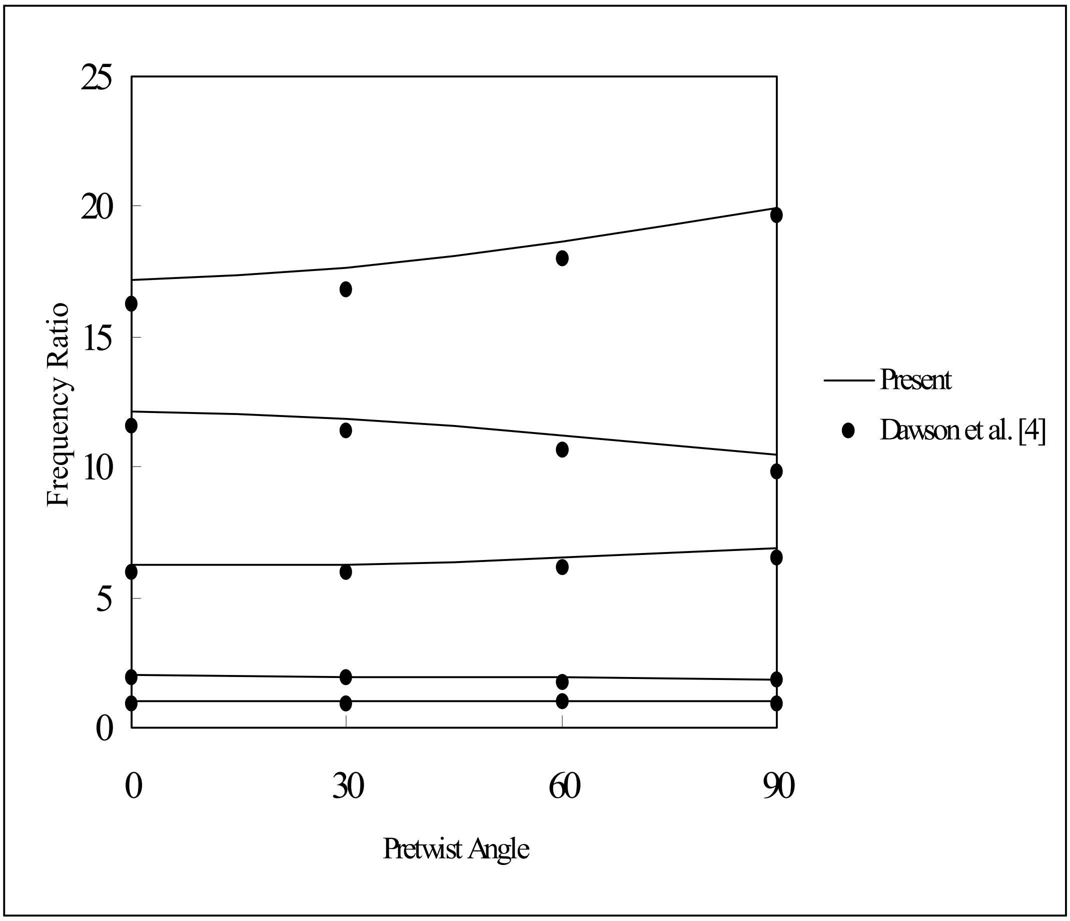

Figure 4.3. Frequency ratio vs twist angle. Length 30.48 cm, breadth 2.54 cm, b/h = 2/1.

Twist Angle	Mode Numbers					Analysis Results
	Frequency Ratio (b/d=8/1), Length=3 in					
	1	2	3	4	5	
0	1,0	6,2	7,4	17,2	33,2	Present (10 Elements)
30	1,0	5,2	8,8	16,8	32,8	
60	1,0	4,1	10,8	15,6	31,8	
90	1,0	3,3	11,8	15,1	29,8	
0	1,0	6,0	7,2	16,7	32,7	Dawson et al. [4]
30	1,0	5,1	8,6	16,0	31,8	
60	1,0	4,0	10,4	14,8	30,3	
90	1,1	3,1	11,4	15,3	28,7	

Table 4.7 Result I for the second group of beams

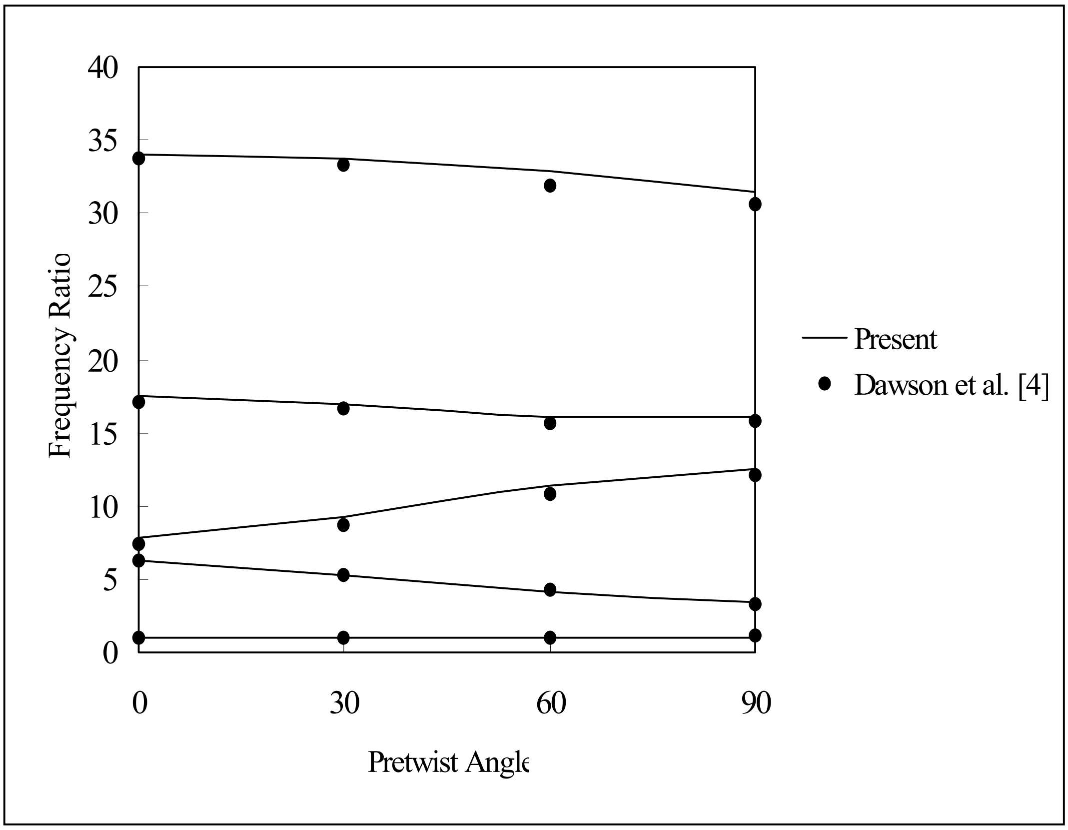

Figure 4.4. Frequency ratio vs twist angle. Length 7.62 cm, breadth 2.54 cm, b/h = 8/1.

Twist Angle	Mode Numbers					Analysis Results
	Frequency Ratio (b/d=8/1), Length=6 in					
	1	2	3	4	5	
0	1,0	6,3	7,8	17,5	34,1	Present (10 Elements)
30	1,0	5,3	9,3	17,0	33,8	
60	1,0	4,2	11,4	16,0	32,9	
90	1,0	3,4	12,6	16,1	31,4	
0	1,0	6,2	7,4	17,1	33,7	Dawson et al. [4]
30	1,0	5,3	8,7	16,7	33,3	
60	1,0	4,3	10,8	15,6	31,9	
90	1,1	3,3	12,1	15,7	30,6	

Table 4.8 Result II for the second group of beams

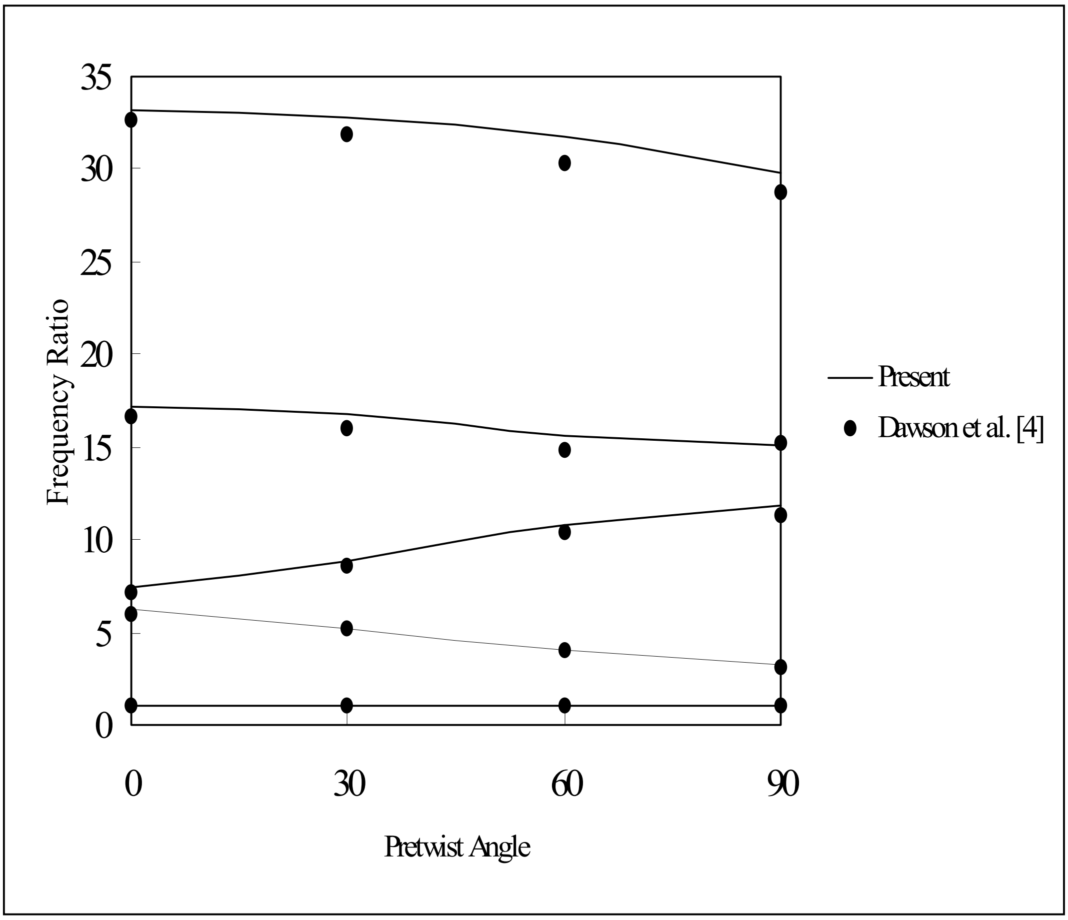

Figure 4.5. Frequency ratio vs twist angle. Length 15.24 cm, breadth 2.54 cm, b/h = 8/1.

Twist Angle	Mode Numbers					Analysis Types
	Frequency Ratio (b/d=8/1), Length=20 in					
	1	2	3	4	5	
0	1,0	6,3	8,0	17,5	34,4	Present (10 Elements)
30	1,0	5,3	9,5	17,1	34,0	
60	1,0	4,2	11,8	16,1	32,9	
90	1,0	3,4	12,8	16,5	31,6	
0	1,0	6,2	8,0	17,6	34,4	Dawson et al. [4]
30	1,0	5,4	9,7	17,0	33,8	
60	1,0	4,3	11,9	16,1	32,6	
90	1,1	3,4	12,8	16,9	31,3	

Table 4.9 Result III for the second group of beams

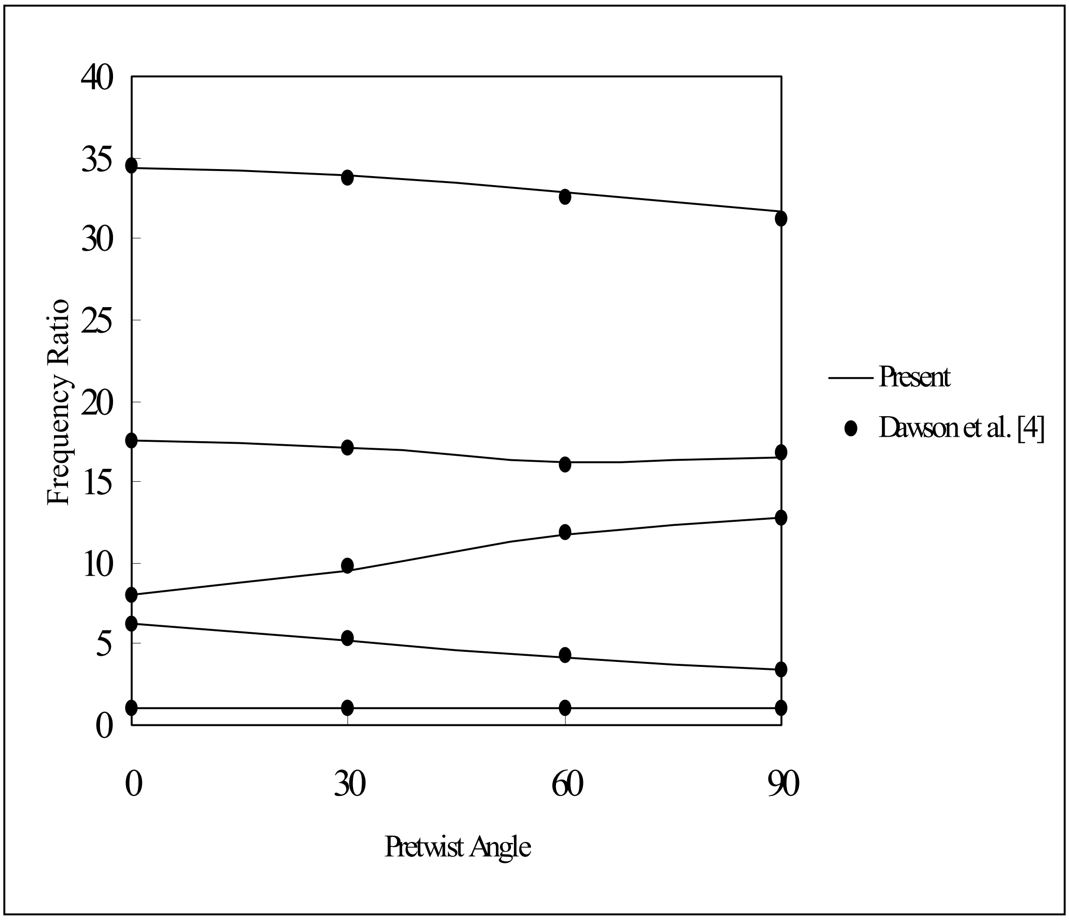

Figure 4.6. Frequency ratio vs twist angle. Length 50.8 cm, breadth 2.54 cm, b/h = 8/1.

4.4 Untwisted rotating cantilever beam

In this example, the case of a rotating untwisted cantilever beam is considered. The first three natural frequencies has been determined and compared with the results of Subrahmanyam and Kulkarni [15] and shown in Table 4.9. The properties of the beam is shown below:

$L = 91.948$ mm

$A = 82.580\ mm^2$

$\rho = 0.0073\ kg/cm^3$

$E = 206.85$ Gpa

$I_{xx} = 577.729\ mm^4$

$w = 540.350$ rad/sec

$r = 263.652$ mm

$G = 82.74$ Gpa

$\kappa = 0.85$

Mode Number	I	II	III
Present	5747.12	33836.19	89263.57
[15]	5608.84	33664.2	87323.28

Table 4.10 Comparison of bending frequencies of an untwisted rotating cantilever beam

The average difference between the present results and the theoretical results [15] is only 1.73 %, it is possible to say that the created FE model shows accurate results even when the rotation effect is included.

4.5 Twisted rotating cantilever beam

Lastly, the accuracy of the present model needs to be confirmed for the twisted rotating cantilever case. The lowest two natural frequencies has been determined and compared with the results of Yoo et al [16] in Table 4.10.

The properties of the beam is shown below:

L = 15 mm

a = 20 mm (breadth)

b = 1 mm (thickness)

ρ = 7830 kg/m^3

E = 206.85 Gpa

T = (ρAL/(EI))

w = γ/T

r = 100 mm

G = 82.74 Gpa

κ = 0.85

θ = 45º

γ	First natural frequency		Second natural frequency	
	Present	Reference[16]	Present	Reference[16]
0.0000	0,1763	0,1763	0,9888	0,9825
0.0882	0,2132	0,2200	1,0209	1,0203
0.1763	0,2963	0,3157	1,1115	1,1253
0.2645	0,3955	0,4288	1,2472	1,2796

Table 4.11 Comparison of natural frequencies of a twisted rotating cantilever beam

An average of 3% difference is observed, it can be also found that the natural frequencies obtained by the present modelling method are lower than those obtained in reference [16]. Thus, the present modeling method provides more accurate results.

Chapter 5

CONCLUSION

A new linearly pretwisted rotating Timoshenko beam finite element, which has two nodes and four degrees of freedom per node, is developed and subsequently used for vibration analysis of pretwisted beams with uniform rectangular cross-section. The finite element model developed is based on two displacement fields that couple the transverse and angular displacements in two planes by satisfying the coupled differential equations of static equilibrium. This procedure means that the rotary inertia term is ignored in the moment equilibrium equation within the element but the effect of rotary inertia will be included in "lumped" form at the nodes.

The present model is verified for various parameters (such as twist angle, length, breadth to depth ratio) in different range on the vibrations of the twisted beam treated experimentally by Carnegie [2] and Dawson et al. [4] and theoretically by other investigators [1, 6, 8, 9, 10, 15, 16] even with ten elements. The new pretwisted both non-rotating and rotating Timoshenko beam element has shown good convergence characteristics and excellent agreement is found with the previous studies. The effects of pretwist angle, beam length and breadth to depth on the natural frequencies are also studied.

REFERENCES

1. R. A. ANDERSON 1953 *Journal of Applied Mechanics* **20**, 504-510. Flexural vibrations in uniform beams according to the Timoshenko theory.
2. W. CARNEGIE 1959 *Proceeding of the Institution of Mechanical Engineers* **173**, 343-374. Vibration of pre-twisted cantilever blading.
3. W. CARNEGIE 1964 *Journal of Mechanical Engineering Science* **6**, 105-109. Vibration of pre-twisted cantilever blading allowing for rotary inertia and shear deflection.
4. B. DAWSON, N. G. GHOSH and W. CARNEGIE 1971 *Journal of Mechanical Engineering Science* **13**, 51-59. Effect of slenderness ratio on the natural frequencies of pre-twisted cantilever beams of uniform rectangular cross-section.
5. R. S. GUPTA and S. S. RAO 1978 *Journal of Sound and Vibration* **56**, 187-200. Finite element eigenvalue analysis of tapered and twisted Timoshenko beams. doi:10.1006/jsvi.2000.3362
6. K. B. SUBRAHMANYAM, S. V. KULKARNI and J. S. RAO 1981 *International Journal of Mechanical Sciences* **23**, 517-530. Coupled bending-bending vibration of pre-twisted cantilever blading allowing for shear deflection and rotary inertia by the Reissner method.
7. A. ROSEN 1991 Applied Mechanics Reviews 44, 843-515. Structural and dynamic behavior of pretwisted rods and beams.
8. W. R. CHEN and L. M. KEER 1993 Journal of Vibrations and Acoustics 115, 285-294. Transverse vibrations of a rotating twisted Timoshenko beam under axial loading.
9. C. K. CHEN and S. H. HO 1999, *International Journal of Mechanical Science* **41**, 1339-1356. Transverse vibration of a rotating twisted Timoshenko beams under axial loading using differential transform.
10. S. M. LIN, W. R. WANG and S. Y. LEE 2001 *International Journal of Mechanical Science* **43**, 2385-2405. The dynamic analysis of nonuniformly pretwisted Timoshenko beams with elastic boundary conditions.

11. J. R. BANERJEE 2001 *International Journal of Solids and Structures* **38**, 6703-6722. Free vibration analysis of a twisted beam using the dynamic stiffness method.
12. S. S. RAO and R. S. GUPTA 2001 *Journal of Sound and Vibration* **242**, 103-124. Finite element vibration analysis of rotating Timoshenko beams.
1. R. NARAYANASWAMI and H. M. ADELMAN 1974 *AIAA Journal* **12**, 1613-1614. Inclusion of transverse shear deformation in finite element displacement formulations.
14. D. J. DAWE 1978 *Journal of Sound and Vibration* **60**, 11-20. A finite element for the vibration analysis of Timoshenko beams.
15. K. B. SUBRAHMANYAM, S. V. KULKARNI and J.S. RAO 1982 *Mechanism and Machine Theory* **17(4)**, 235-241. Analysis of lateral vibrations of rotating cantilever blades allowing for shear deflection and rotary inertia by Reissner and potential energy methods.
16. H. H. YOO, J.Y. KWAK and J. CHUNG 2001 *Journal of Sound and Vibration* **240(5)**, 891-908. Vibration Analysis of rotating pretwisted blades with a concentrated mass.
17. M. PETYT 1990 *Introduction to Finite Element Vibration Analysis*. Cambridge: Cambridge University Press.
18. K. J. BATHE 1996 *Finite Element Procedures.* New Jersey, Prentice Hall.
19. T. R. CHANDRUPATLA and A. D. BELEGUNDU 1997 *Introduction to Finite Elements in Engineering.* New Jersey, Prentice-Hall, Inc.
20. W. T. THOMSON 1988 *Theory of Vibration and Applications*. New Jersey, Prentice-Hall, Inc.
21. J. S. RAO 1991 *Turbomachine Blade Vibration.* Wiley Eastern Limited, New Delhi, India.
22. W. WEAVER, S. P. TIMOSHENKO, D. H. YOUNG 1990 *Vibration Problems in Engineering*. John Wiley & Sons, Ltd.
23. WWW Page of eFunda, Inc. *The ultimate online reference for engineers*. (www.efunda.com)